A dark matter disc in three cosmological simulations of Milky Way mass galaxies

J. I. Read,[1][*] L. Mayer,[1] A. M. Brooks,[2] F. Governato[3] and G. Lake[1]

[1]*Institute for Theoretical Physics, University of Zurich, Winterthurerstrasse 190 8047, Switzerland*

[2]*California Institute of Technology, M/C 130-33, Pasadena, CA 91125, USA*

[3]*Astronomy Department, University of Washington, Box 351580, Seattle, WA 98195-1580, USA*

ABSTRACT

Making robust predictions for the phase-space distribution of dark matter at the solar neighbourhood is vital for dark matter direct-detection experiments. To date, almost all such predictions have been based on simulations that model the dark matter alone. Here, we use three cosmological hydrodynamic simulations of bright, disc-dominated galaxies to include the effects of baryonic matter self-consistently for the first time. We find that the addition of baryonic physics drastically alters the dark matter profile in the vicinity of the solar neighbourhood. A stellar/gas disc, already in place at high redshift, causes merging satellites to be dragged preferentially towards the disc plane where they are torn apart by tides. This results in an accreted dark matter disc that contributes $\sim$0.25–1.5 times the non-rotating halo density at the solar position. The dark disc, unlike dark matter streams, is an equilibrium structure that must exist in disc galaxies that form in a hierarchical cosmology. Its low rotation lag with respect to the Earth significantly boosts Weakly Interacting Massive Particle (WIMP) capture in the Earth and Sun, boosts the annual modulation signal and leads to distinct variations in the flux as a function of recoil energy that allow the WIMP mass to be determined.

Key word: dark matter.

1 INTRODUCTION

The case for dark matter in the Universe is based on a wide range of observational data from galaxy rotation curves and gravitational lensing to the cosmic microwave background radiation (e.g. de Blok et al. 2001; Clowe et al. 2006; Read, Saha & Macciò 2007; Dunkley et al. 2009). Of the many plausible dark matter candidates in extensions to the Standard Model, Weakly Interacting Massive Particles (WIMPs) stand out as well motivated and detectable (Jungman, Kamionkowski & Griest 1996), giving rise to many experiments designed to detect WIMPs in the lab (Aprile et al. 2005; Bernabei et al. 2008; Ahmed et al. 2009). Predicting the flux of dark matter particles through the Earth is key to the success of such experiments, both for motivating detector design and for the interpretation of any future signal (Jungman et al. 1996).

Most previous works have modelled the distribution of dark matter at the solar neighbourhood using, or extrapolating from, cosmological simulations that model only the dark matter (Kamionkowski & Koushiappas 2008; Kuhlen, Diemand & Madau 2008; Stadel et al. 2008; Springel et al. 2008; Vogelsberger et al. 2008a,b; Zemp et al. 2009). These exquisitely describe the amount and properties of dark matter substructure. But they do not model the baryonic component of the Milky Way that presently dominates the mass interior to the solar radius (Dehnen & Binney 1998; Klypin, Zhao & Somerville 2002; Widrow & Dubinski 2005) and likely did so since redshift $z = 1$, when the mean merger rate in a ΛCDM cosmology peaked (Gottlöber, Klypin & Kravtsov 2001; Dalcanton & Bernstein 2002; Bensby et al. 2007; Kampczyk et al. 2007).

In recent work, we demonstrated that the Milky Way stellar/gas disc is important because it biases the accretion of satellites, causing them to be dragged towards the disc plane (Read et al. 2008). As these satellites are torn apart by tidal forces, their accreted material settles into a thick disc of stars and dark matter (Lake 1989; Read et al. 2008). The dark disc, unlike dark matter streams, is an equilibrium structure that must exist in disc galaxies that form in a hierarchical cosmology. Its low rotation lag with respect to the Earth significantly boosts WIMP capture in the Earth and Sun (Bruch et al. 2008b, 2009), boosts the annual modulation signal and leads to distinct variations in the flux as a function of recoil energy that allow the WIMP mass to be determined[1] (Bruch et al. 2008a).

---

[1] These conclusions do depend on the particular WIMP model. The dark disc has a strong effect for dark matter that scatters elastically, for example, but a weaker effect for 'inelastic' dark matter (see e.g. March-Russell, McCabe & McCullough 2008).

[*]E-mail: justin@physik.uzh.ch

Table 1. Simulation labels and parameters.

Simulation	$(\Omega_m, \Omega_\Lambda, \sigma_8, h)$	$(N_{dm}, N_*, N_{gas})/10^6$	$\min(M_{dm}, M_*, M_{gas})/10^5\,\mathrm{M_\odot}$	$\epsilon_{dm,*,gas}/\mathrm{kpc}$	$M_{dm}^{<300\,\mathrm{kpc}}/10^{12}\,\mathrm{M_\odot}$
MW1	(0.3, 0.7, 0.9, 0.7)	(2.8, 3.1, 1.5)	(7.6, 0.2, 0.3)	0.3	1.1
H204	(0.24, 0.76, 0.77, 0.73)	(4, 3.3, 1.7)	(10.1, 0.41, 0.58)	0.35	0.8
H258	(0.24, 0.76, 0.77, 0.73)	(3.5, 2.2, 1.4)	(10.1, 0.35, 0.58)	0.35	0.75
H258dark	(0.24, 0.76, 0.77, 0.73)	(3.5, −, −)	(12.25, −, −)	0.35	0.9

Note. From left to right: the columns show the simulation label, the cosmological parameters used, the number of dark, star and gas particles at redshift $z = 0$, the minimum dark matter, star and gas particle masses at $z = 0$, the dark matter, star and gas force softenings (these are always equal) and the dark matter mass within 300 kpc at $z = 0$. H258dark was set up with the same initial conditions as H258, but run with only dark matter particles, and at slightly lower mass resolution.

In Read et al. (2008), we used dark matter only simulations to quantify the expected merger history for Milky Way mass galaxies in ΛCDM and a series of isolated collisionless satellite–Milky Way merger simulations to estimate the expected properties of the dark disc. We found that, for plausible merger histories, the dark disc contributes ∼0.25–1 times the halo density at the solar neighbourhood. In this paper, we make the first attempt to include the baryonic matter self-consistently, using three ΛCDM cosmological hydrodynamic simulations of Milky Way mass galaxies. Both approaches are complementary in quantifying the expected properties of the dark disc. Our previous approach allowed us to precisely specify the properties of the Milky Way disc and its merging satellites at high redshift; our current approach is fully self-consistent. We model the radiative cooling, star formation and feedback physics that lead to the formation of realistic disc galaxies in their cosmological context. Recent improvements in such simulations have made it possible to form galaxies with a significant disc component and reproduce some basic galaxy properties over a range of redshifts (Governato et al. 2007; Scannapieco et al. 2008; Zavala, Okamoto & Frenk 2008; Pontzen et al. 2008). Due to the stochastic nature of galaxy assembly in ΛCDM, and our limited sample of simulated galaxies, we do not attempt to form genuine Milky Way analogues. Instead, we choose three galaxies with mass comparable to that of the Milky Way which span a range of interesting assembly histories. We infer plausible dark disc properties for the Milky Way from these simulations.

This paper is organized as follows. In Section 2, we describe the state-of-the-art cosmological hydrodynamic simulations. In Section 3, we present our results. In Section 4, we discuss our numerical limitations and the implications of our results for the Milky Way. Finally, in Section 5, we present our conclusions.

2 THE COSMOLOGICAL HYDRODYNAMIC SIMULATIONS

We use three cosmological hydrodynamic simulations of Milky Way mass galaxies, two of which (MW1, H258) have already been presented in Brooks et al. (2007, 2009), Mayer, Governato & Kaufmann (2008), Governato, Mayer & Brook (2008a) and Governato et al. (2008b). All three were run with the GASOLINE code (Wadsley, Stadel & Quinn 2004) using 'blastwave feedback' (Stinson et al. 2006); the simulation labels, parameters and choice of cosmology are given in Table 1. We also ran a fourth simulation, H258dark. This had the same initial conditions as H258, but was run with only dark matter particles, and at slightly lower mass resolution. (Note that since the matter density of the Universe Ω_m is fixed, the dark matter density is higher in H258dark than in H258.) The final outputs were mass and momentum centred using the 'shrinking-sphere' method described in Read et al. (2006a), and

rotated into their moment of inertia eigenframe with the z-axis perpendicular to the disc. For MW1, H204 and H258, the eigenframe was found using the stars; for H258dark it was found using the dark matter.

The three galaxies were selected from two 50 Mpc uniform volume simulations as part of a large sample that spans the typical range in spin and formation times for dark matter haloes of mass ∼$10^{12}\,\mathrm{M_\odot}$. Their halo mass is that associated with L_* galaxies; their local density within 10 Mpc was close to average such that all three are 'field' galaxies, and their spin parameters bracket the cosmological mean. None of the galaxies was specifically selected to be a Milky Way analogue. Instead, we selected three galaxies of comparable mass to the Milky Way, but spanning a range of interesting merger histories. MW1 had a very quiescent merger history, with no major mergers after redshift $z = 2$; H204 had several massive mergers after redshift $z = 1$ and H258 was an extreme case with a very massive ∼1:1 merger at $z = 1$. In Section 4, we discuss which of these is most like our Galaxy.

The analysis was performed as in Read et al. (2008). The subhaloes inside each host galaxy and at each redshift output were identified using the Amiga Halo Finder (AHF[2]) algorithm (Gill, Knebe & Gibson 2004). The subhaloes were then traced backwards in time. To avoid ambiguities in this halo tracking, we ordered subhaloes by mass so that subhaloes were linked to their most massive progenitor not already claimed by a larger subhalo. A final complication can occur if two subhaloes are about to merge. In such a situation, AHF sometimes overestimates the mass of the smaller of the two. We dealt with this problem by searching for sudden spikes in mass at pericentre and removing these by assigning the mass found at the previous output time. We define a subhalo as merged (disrupted) if it has less than a tenth of its peak circular speed considered over all times. Our results are not sensitive to this parameter.

3 RESULTS

3.1 Forming a disc of dark matter

Figs 1(a)–(c) show the distribution of rotational velocities v_ϕ at the solar neighbourhood ($7 < R < 8$ kpc; $|z| < 2.1$ kpc) for the stars (red) and dark matter (black) in MW1, H204 and H258. Overplotted in panel (c) is the distribution for H258dark, modelled with dark matter alone (black dotted). Our results are not sensitive to the position of the 'solar neighbourhood' slice (a choice of $5.5 < R < 6.5$ kpc gave near-identical results). With the exception of H258dark, all of the dark matter distributions are skewed towards
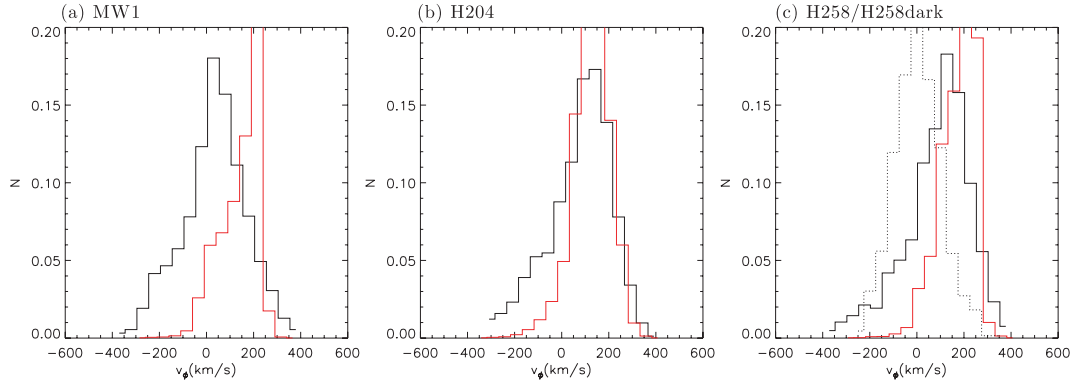
---

[2] http://www.aip.de/People/AKnebe/AMIGA/

Figure 1. (a–c) The distribution of rotational velocities at the solar neighbourhood ($7 < R < 8$ kpc; $|z| < 2.1$ kpc) for three simulated Milky Way mass galaxies MW1, H204 and H258. The lines show the dark matter (black) and stars (red). The dark matter distribution for H258dark, simulated with *dark matter alone*, is overplotted on (c) (black dotted).
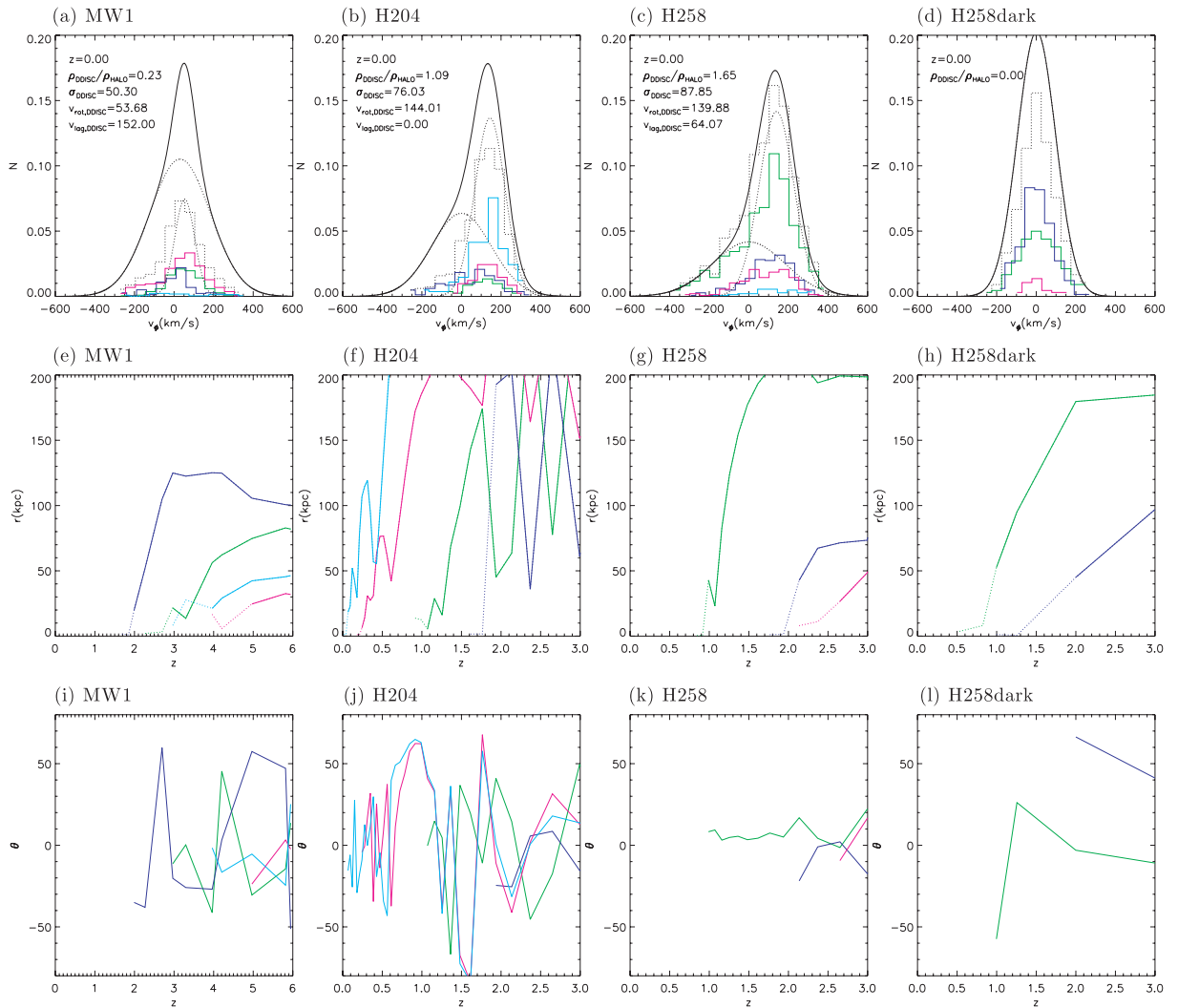

Figure 2. (a–c) The decomposed distribution of rotational velocities at the solar neighbourhood ($7 < R < 8$ kpc; $|z| < 2.1$ kpc) for three simulated Milky Way mass galaxies MW1, H204 and H258. The lines show a double-Gaussian fit to the dark matter (black; black dotted), the dark matter accreted from the four most massive disrupted satellites (green, blue, magenta, cyan) and the sum of all dark matter accreted from these satellites (black dotted histogram). The best-fitting double-Gaussian parameters are marked in the top left, along with the redshift, z. (d) As in (a–c), but for the galaxy H258 simulated with *dark matter alone*. (e–h) The decay in radius r as a function of redshift z of the four most massive disrupting satellites in MW1, H258 and H258dark. Where less than four lines are shown, these satellites accreted at redshift $z > 3$. The dotted sections show the evolution of the most bound particle in the satellite after the satellite has disrupted. (i–l) The decay in angle to the Milky Way stellar disc, θ, as a function of redshift, z, of the four most massive disrupting satellites in MW1, H204, H258 and H258dark.

the stars. Figs 2(a)–(d)show a decomposition of these distributions. All three baryonic simulations require a double-Gaussian fit to their dark matter v_ϕ distribution (smooth black and black dotted lines). The second Gaussian rotates rapidly and matches well the material accreted from the sum of the four most massive satellites (black dotted histogram), though our fit did not require this. (Nor did our fit require either Gaussian to have mean rotational velocity $\overline{v_\phi} = 0$.) It is this accreted, rapidly rotating material that we call the 'dark disc'.

Figs 2(a)–(d) show how the material accreted from the four most massive merging satellites[3] (green, blue, magenta and cyan) contributes to the dark disc for MW1, H204 and H258. Figs 2(e)–(h) show the decay in radius as a function of redshift z of these satellites, and Figs 2(i)–(l) show the decay in angle θ to the host galaxies' disc as a function of redshift z.

The mass and rotation speed of the dark disc increase in the simulations with more late mergers. MW1 has no significant mergers after redshift $z = 2$ and has a less significant dark disc, with a rotation lag with respect to the stars (red lines in Fig. 1) of ~ 150 km s^{-1}, and dark disc to halo density ratio of $\rho_{DDISC}/\rho_{HALO} = 0.23$ (obtained from the double-Gaussian fit). H204 and H258 both have extreme dark discs with $\rho_{DDISC}/\rho_{HALO} > 1$ and a rotation lag with respect to the stars of $\lesssim 60$ km s^{-1}; they both have massive mergers at redshift $z < 1$.

Figs 2(i)–(j) demonstrate that disc-plane dragging is responsible for the formation of the dark disc in MW1 and H204. In MW1, the green satellite is dragged towards the disc plane, the magenta and cyan satellites start out close to the disc plane and the blue satellite merges at high inclination angle. Fig. 2(a) shows the contribution to the dark disc owing to each of these satellites. The magenta satellite contributes the most, being both low-inclination and massive, followed by the green. The cyan satellite is of too low mass to contribute significantly, while the blue satellite contributes little rotating material because of its high inclination. These results confirm our expectations from isolated disc–satellite merger simulations (Read et al. 2008). Similar results can be seen for the four most massive mergers in H204. Although initially on high inclination orbits, the magenta and cyan satellites complete enough pericentre passages to be dragged down into the disc plane and contribute significantly to the dark disc. The blue and green satellites also contribute in equal measure, though somewhat less than the magenta and cyan satellites owing to their higher final inclinations.

H258 presents an interesting special case. Its green satellite is a near 1:1 low inclination merger that comprises almost all of the resulting dark disc. Since the green satellite is initially low inclination, disc-plane dragging plays no role in the formation of this dark disc. Yet the same simulation run without any baryons – H258dark – has no dark disc. This suggests that the baryons still play an important role – extra to disc-plane dragging – in H258. We discuss this in Section 3.2.

It is interesting that in all three galaxies, none of the four most massive satellites contributes significant retrograde material at the solar neighbourhood. This is surprising given that dark matter only simulations show only a small prograde bias in the satellite distribution about the spin axis of the dark matter halo (Warnick & Knebe 2006). We will investigate this further in a forthcoming paper, but note here that retrograde mergers are suppressed because of reduced dynamical friction (Quinn & Goodman 1986; Read et al. 2008) and reduced tidal forces (Read et al. 2006b). Both of these effects will

cause material accreted from a retrograde merger to be deposited at larger radii than that from the equivalent prograde merger. This can explain a prograde bias in accreted material at the solar neighbourhood without requiring a similarly strong bias in the satellite orbit distribution.

3.2 Maintaining the dark disc: the importance of halo shape

Figs 3(e)–(h) show projected density contours for the total dark matter (black) and the dark matter accreted from the four most massive satellites (black dotted), in MW1, H204, H258 and H258dark. All of the simulations that include the baryons produce near-spherical, slightly oblate, final dark matter density distributions that have symmetry axes parallel to the stellar disc. This agrees well with previous numerical results in the literature (Kazantzidis et al. 2004; Debattista et al. 2008). Indeed, observations of the Sagittarius stream of stars suggest that the Milky Way has a near-spherical halo with axis ratio $a/c \gtrsim 0.9$ within ~ 50 kpc (Johnston, Law & Majewski 2005; Fellhauer et al. 2006). Of our three simulated galaxies, only the most flattened case, H204, with an axis ratio $a/c \sim 0.77$ within ~ 50 kpc, is inconsistent with the Milky Way. By contrast, without the baryons, the dark matter halo in H258dark is highly triaxial (Fig. 3h). Indeed, the typical dark matter halo in ΛCDM simulations that model the dark matter alone is triaxial, prolate and inconsistent with observations of the Milky Way (Macciò et al. 2007).

As noted above, both H258 and H258dark have ~ 1:1 mergers at redshift $z \sim 1$. In H258 this merger produces a dark disc, but in H258dark it does not. Since mergers of this mass ratio define the post-merger plane of the disc, the difference cannot be due to disc-plane dragging. Instead, the difference is due to the halo shapes. In a static oblate potential such as that in H258, particles conserve the z-component of their angular momentum vector. Any sense of rotation established in the merger will be preserved. By contrast, in a static triaxial potential like that in H258dark, particles moving on regular orbits do not explicitly conserve any component of their angular momentum vector. Their orbit planes precess and any sense of rotation established in the merger is rapidly lost. As a result, the final velocity distribution at the solar neighbourhood in H258dark is a Gaussian. This demonstrates that in addition to disc-plane dragging, the near-spherical halo that results once the baryons are included is a vital ingredient in the formation and survival of a dark matter disc.

3.3 The mass and spatial distribution of the dark disc

The precise properties of the dark disc depend on how we decompose the total dark matter distribution into 'disc' and 'halo' components. We choose a decomposition where the dark disc is the material that originates from the innermost 5 per cent of the four most massive merging satellites. This gives the best match to the highly rotating Gaussian component in our double-Gaussian fit to the local dark matter velocity distribution (see Fig. 2).

Figs 3(a)–(d) show the mean streaming velocities ($\overline{v_\phi}$ averaged in bins $\Delta R = 1$ kpc) for the stars (red) and gas (red dotted) in a slice $|z| < 1.1$ kpc for MW1, H204, H258 and H258dark. Overplotted are the circular velocity profiles (computed from the enclosed mass) for the dark matter (black), the sum of dark matter accreted from the four most massive satellites (black dotted) and the sum of dark matter accreted from the inner 5 per cent of the four most massive satellites (black dashed). Using our above decomposition, the dark disc contributes at most half of the rotation curve at the solar neighbourhood (in H258). Since the rotation curve goes as the square

---

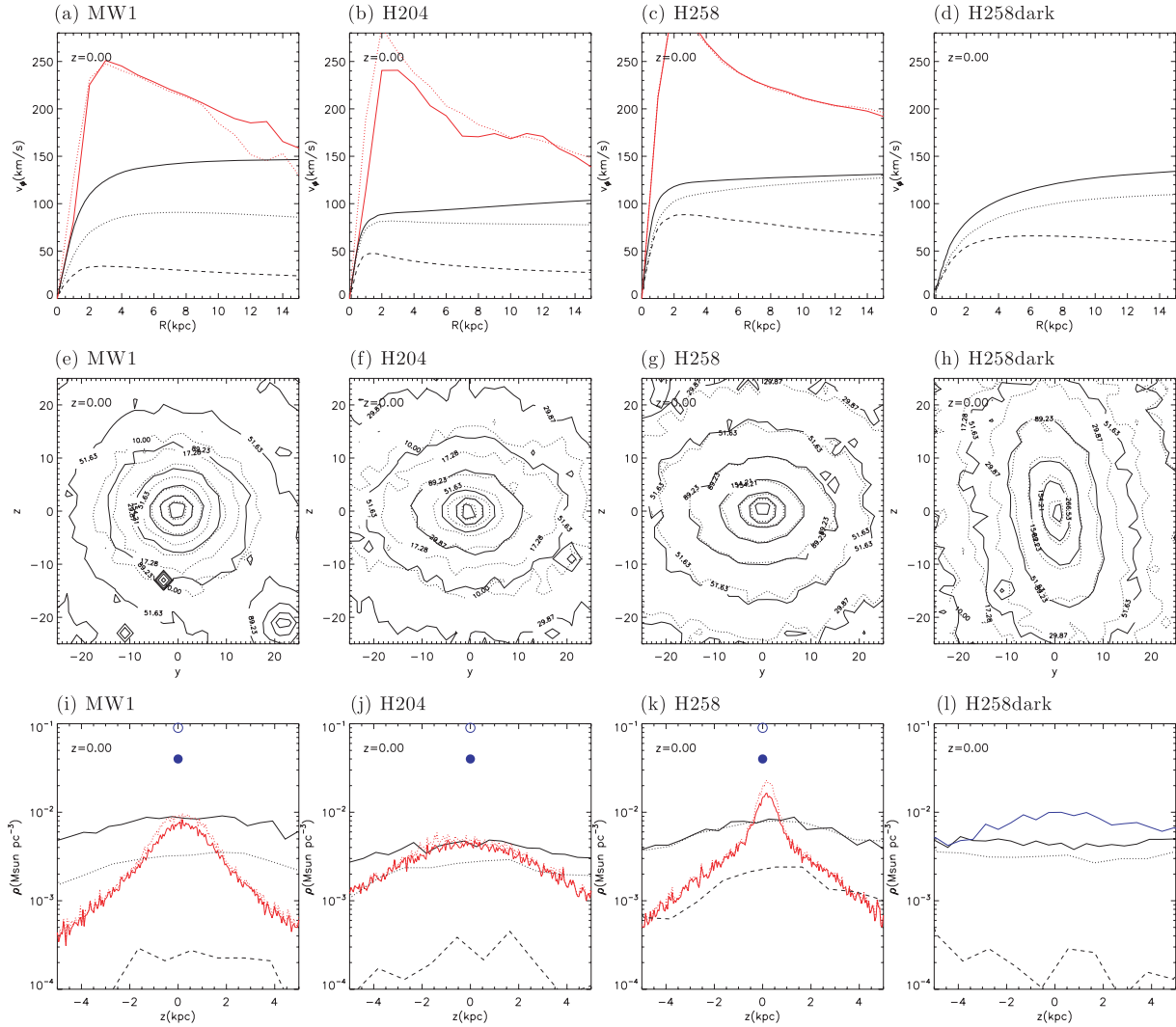[3] Considered over their whole lifetime.

Figure 3. (a–d) The mean streaming velocities for the young stars (red) and gas (red dotted) in a slice $|z| < 1.1$ kpc for MW1, H204, H258 and H258dark. Overplotted are the circular velocity profiles (computed from the enclosed mass) for the dark matter (black), the sum of dark matter accreted from the four most massive satellites (black dotted) and the sum of dark matter accreted from the inner 5 per cent of the four most massive satellites (black dashed). (e–h) Projected density contours for the dark matter (black) and the sum of dark matter accreted from the four most massive satellites (black dotted). (i–l) Density of stars (red), stars + gas (red dotted), dark matter (black) and dark matter accreted from the four most massive satellites [black dotted and dashed as in (a–d)] as a function of height z in a slice $7 < R < 8$ kpc for MW1, H204, H258 and H258dark. For MW1, H204, H258, we overplot the observed star (solid blue circle) and star+gas (open blue circle) stellar density in the solar neighbourhood for the Milky Way (taken from Holmberg & Flynn 2000). For H258dark, we show the profile for the alignment given in panel (h) (black), and one rotated by 90° to this about the x-axis (blue).

root of the mass, this is a quarter of the mass. The other extreme is MW1 where the dark disc contributes a fifth of the rotation curve at the solar neighbourhood.

Figs 3(i)–(l) show the density of stars (red), dark matter (black), dark matter accreted from the four most massive satellites (black dotted) and dark matter accreted from the inner 5 per cent of the four most massive satellites (black dashed) as a function of height z in a slice $7 < R < 8$ kpc for MW1, H204, H258 and H258dark. In MW1, H204 and H258 the density profile is peaked, indicating a disc-like structure – particularly for the inner 5 per cent distributions. In H258dark, the profile depends on our choice of alignment. In its eigenframe, $\rho(z)$ is flat, as expected for a more spheroidal dark matter distribution. In a frame rotated by 90° to this about the x-axis, however, the distribution is peaked similarly to H258 (blue line; Fig. 3l). However, there is no measurable rotation in the dark matter v_ϕ distribution for H258dark for any alignment. The peaky

$\rho(z)$ distribution in H258dark is the result of a flattened halo, not a dark disc. For our above decomposition, the dark disc in MW1, H204 and H258 is a structure that rotates in the same sense as the stellar disc and is flattened in the same plane as the stellar disc – hence the name 'dark disc'.

3.4 Observing the dark disc

Fig. 4 shows a comparison of the star (red) and dark matter (black) velocity distributions at the solar neighbourhood ($7 < R < 8$ kpc; $|z| < 2.1$ kpc) of material accreted from the four most massive disrupted satellites in MW1, H204 and H258. Also plotted is the dark matter accreted from the inner 5 per cent of these satellites (dotted line). The accreted stars comprise 5, 40 and 30 per cent of the stars in the solar neighbourhood for MW1, H204 and H258,
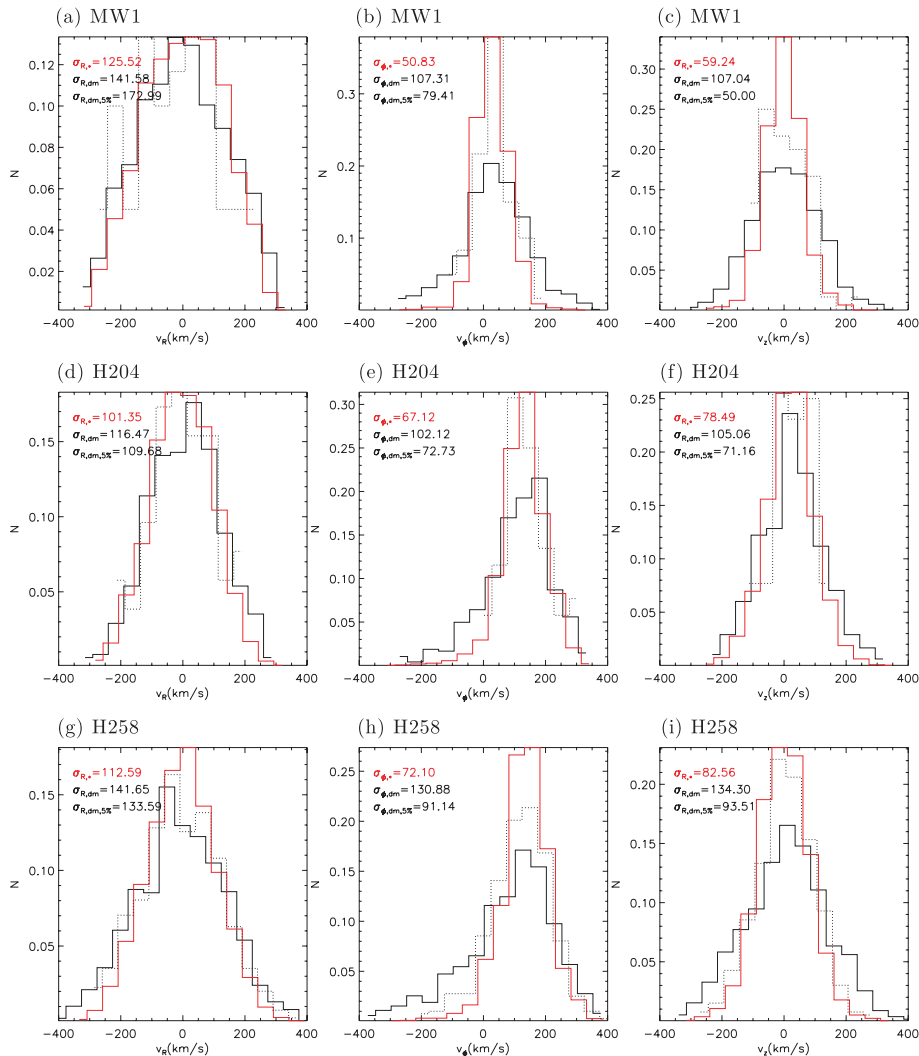
Figure 4. (a–d) A comparison of the accreted star (red) and accreted dark matter (black) velocity distributions v_R (left hand panel), v_ϕ (middle) and v_z (right hand panel) at the solar neighbourhood ($7 < R < 8\,\mathrm{kpc}$; $|z| < 2.1\,\mathrm{kpc}$), for MW1, H204 and H258. We plot the sum of material accreted from the four most massive disrupted satellites. Also plotted is the dark matter coming from the inner 5 per cent of these satellites (dotted lines). The dispersions are given in the top-left corner of each plot in km s^{-1}.

respectively (see Brook et al., in preparation, for a study on the decomposition of these into bulge, disc and halo stars). The accreted stars are colder than the full accreted dark matter distributions, but close to the inner 5 per cent dark matter distribution. The best-fitting parameters for the dark disc (see Figs 2a–d) lie close to both the stellar distributions and the inner 5 per cent dark matter distributions. If future surveys of our Galaxy can disentangle accreted stars in the Milky Way thick disc from those that formed in situ, then we will be able to infer, through numerical modelling, the velocity distribution function of the dark disc from these stars. We will investigate this in more detail in future work, but note here that the galaxy with the most quiescent merger history (MW1) has an accreted star fraction in the solar neighbourhood that is quite small. In the Milky Way, for example, these accreted stars would contribute at most only half of the mass of the Milky Way thick stellar disc (Jurić et al. 2008). If the accreted stars form only a small fraction of the Milky Way thick disc, finding them will require high-quality data that combine six-dimensional phase-space information with detailed chemical tagging. This will become available with next generation Galactic surveys (see e.g. Perryman et al. 2001).

4 DISCUSSION: THE IMPORTANCE OF BARYONS

Several recent studies have highlighted the importance of baryons for the global dark matter distribution, finding that baryons cause dark matter haloes to contract (e.g. Gnedin et al. 2004; Pedrosa, Tissera & Scannapieco 2009; Romano-Diaz et al. 2009) and to change shape (e.g. Kazantzidis et al. 2004; Debattista et al. 2008; Abadi et al. 2009). Here, we have focused on the effect of baryonic discs on the *local* dark matter distribution. As in these earlier studies, we find that once the stars and gas are included, dark matter haloes become significantly rounder. However, in addition, we find that the star/gas disc – already in place at high redshift – biases the accretion of massive satellites, preferentially dragging them towards the disc plane. Both effects combined lead to a solar neighbourhood velocity distribution that is anisotropic, and a better fit in v_ϕ by a double-Gaussian than a single Gaussian. The highly rotating second Gaussian component is what we call the *dark matter disc*.

It is not clear which of MW1, H204 or H258 provides the best match to our Galaxy. The Milky Way has evidence for several

mergers since $z \sim 1$. The Sagittarius dwarf recently fell in on a polar orbit (Ibata, Gilmore & Irwin 1994; Majewski et al. 2003). There is evidence for a merger in the plane of the disc (Conn et al. 2007), and another $\lesssim 5$ Gyr ago from the chemistry and kinematics of stars in the solar neighbourhood (Feltzing & Bensby 2008). Finally, the Milky Way thick disc itself is evidence for an $\sim 1{:}10$ merger at $z \sim 1$ (Kazantzidis et al. 2008; Read et al. 2008). MW1 had no significant mergers after $z \sim 2$ and is likely overquiescent as compared to our Galaxy. By contrast, both H204 and H258 appear to have merger histories that are too extreme as compared with the Milky Way. This results in large fractions (30–40 per cent) of accreted stars at the solar neighbourhood. Assuming all stars in the Milky Way thick disc are accreted gives an upper bound of 12 per cent for our Galaxy (Jurić et al. 2008).

However, differences between the simulated galaxies and the Milky Way could also be a result of numerical limitations. All three state-of-the-art simulations have a force softening of ~ 300 pc, which is larger than the measured scaleheight of the Milky Way thin stellar disc (Jurić et al. 2008); spurious angular momentum loss occurring in underresolved progenitors may have still affected the final mass distribution even at the high-mass resolution employed here (Mayer et al. 2008); the sub-grid physics scheme is a source of systematic error (Mayer et al. 2008) and the smoothed particle hydrodynamics technique employed does not correctly resolve fluid instabilities and mixing[4] (Agertz et al. 2007).

Owing in part to these limitations in the numerics, and in part to the fact that the initial conditions were not chosen specifically to reproduce the structure and assembly history of the Milky Way suggested by observational constraints, the comparison with the Milky Way has to be done with caution. Indeed, the simulated galaxies more closely resemble L_* Sa galaxies than a Milky Way-like Sb/Sc galaxy, as shown by their location in the Tully–Fisher relation (Governato et al. 2008a). They have a larger bulge-to-disc ratio relative to the Milky Way (Mayer et al. 2008), $B/D \sim 0.5$–0.65 (measured both photometrically and kinematically; see Governato et al. 2007, 2008a), rather than the 0.2–0.3 measured for the Milky Way, a more massive stellar halo and a lower gas fraction in the disc. As a result, while the total baryonic mass of these galaxies is comparable to that of the Milky Way, the stellar disc mass is a factor of 2–3 lower than that of the disc of the Milky Way, and the gas mass in the disc is lower by an even greater factor. The lower disc mass combined with the effect of softening, that tends to smear out physical density, yields a stellar volume density lower by a factor of ~ 3.5 compared to the stellar density of the Milky Way at the solar neighbourhood and a total baryonic (star+gas) density in the disc plane lower by a factor of ~ 10 at the same radius (Holmberg & Flynn 2000; see Figs 3i–l). Due to the same structural differences, in particular to the larger bulge-to-disc ratio, the mean streaming velocity also falls with radius faster than in the Milky Way (Figs 3a–d). This will cause disc-plane dragging – and therefore the mass of the dark disc – to be underestimated.[5]

Despite these numerical and observational limitations, our qualitative results are robust. Dark disc formation is a gravitational process that requires just three key ingredients to be modelled correctly: (i) having a stellar/gas disc in place at high redshift as observed in real galaxies; (ii) having a dark matter halo that is oblate and aligned with the stellar disc and (iii) having a merger history given by our current ΛCDM cosmology. All three are satisfied by our simulations.

With the above limitations in mind, we tentatively suggest that the Milky Way is intermediate between simulations MW1 and H204. Future simulations that better resolve the Milky Way and its satellites and that are tuned to reproduce the Milky Way's merger history will provide improved constraints.

5 CONCLUSIONS

Predicting the local phase-space density of dark matter is central to efforts to directly detect dark matter, both to motivate detector design and to interpret any future signal. Previous efforts to estimate this have used simulations that model the dark matter alone. In this paper, we used three state-of-the-art ΛCDM cosmological hydrodynamic simulations of Milky Way mass galaxies to include the stars and gas self-consistently for the first time. Our main findings are as follows.

(i) Once the stars and gas are included, the dark matter haloes become significantly rounder, while the stellar/gas disc biases the accretion of massive satellites, dragging them towards the disc plane. Both effects combined lead to the formation of a dark matter disc with ~ 0.25–1.5 times the halo density at the solar neighbourhood, in excellent agreement with a previous estimate obtained using different methodology (Read et al. 2008). The resulting solar neighbourhood dark matter velocity distributions are anisotropic, and better fit in v_ϕ by a double-Gaussian than a single Gaussian. The highly rotating second Gaussian component is the 'dark disc'. We found a rotation lag compared to the Milky Way stellar disc in the range: $v_{\mathrm{lag}} \sim 0$–150 km s^{-1}.

(ii) Our three Milky Way mass galaxies were chosen to span a range of interesting merger histories, not to be precise replicas of the Milky Way. We found that more late mergers gave rise to a more significant dark disc. The Milky Way likely has a dark disc intermediate between our most quiescent galaxy and our second most quiescent galaxy. This suggests a local dark disc density of ~ 0.23–1 times the non-rotating halo density, and a rotation lag with respect to the Milky Way's stellar disc of $v_{\mathrm{lag}} = 0$–150 km s^{-1}. Increased resolution and cosmological models that better capture the structural properties of the Milky Way will give improved constraints. For median values of $\rho_{\mathrm{DDISC}}/\rho_{\mathrm{HALO}} \sim 0.5$ and $v_{\mathrm{lag}} \sim 50$ km s^{-1}, the dark disc boosts WIMP capture in the Earth and Sun (Bruch et al. 2008b, 2009), enhances the annual modulation signal and leads to distinct variations in the flux as a function of recoil energy that allow the WIMP mass to be determined (Bruch et al. 2008a).

(iii) An accreted disc of stars forms concurrent with the dark disc and shares similar kinematics. If future surveys of our Galaxy can disentangle accreted stars in the Milky Way thick disc from those that formed in situ, then we will be able to infer, through numerical modelling, the velocity distribution function of the dark disc from these stars. We will investigate this further in our future work.

---

[4] This is not likely to be the main source of error, however, since instabilities mostly affect the interstellar medium that is in any case poorly resolved.

[5] There is a competing effect that has the opposite sign: the merging satellites are themselves overconcentrated due to the same numerical limitations. This causes the dark matter, through adiabatic contraction, to be overconcentrated also. This has two effects. First, the satellites are more resilient to tides and more able to get down into the disc. Secondly, there is more dark matter at small radii within the satellites. Both effects will act to overestimate the dark disc mass. However, even without any baryons, H258dark has significant contributions from its accreted satellites at small radii (compare Figs 3c and d, dotted and dashed lines). This suggests that this effect is small.

REFERENCES

Abadi M. G., Navarro J. F., Fardal M., Babul A., Steinmetz M., 2009, preprint (arXiv:0902.2477)
Agertz O. et al., 2007, MNRAS, 380, 963
Ahmed Z. et al. (CDMS Collaboration), 2009, Phys. Rev. Lett., 102, 011301
Aprile E. et al., 2005, New Astron. Rev., 49, 289
Bensby T., Zenn A. R., Oey M. S., Feltzing S., 2007, ApJ, 663, L13
Bernabei R. et al., 2008, Eur. Phys. J. C, 56, 333
Brooks A. M., Governato F., Booth C. M., Willman B., Gardner J. P., Wadsley J., Stinson G., Quinn T., 2007, ApJ, 655, L17
Brooks A. M., Governato F., Quinn T., Brook C. B., Wadsley J., 2009, ApJ, 694, 396
Bruch T., Read J., Baudis L., Lake G., 2008a, preprint (arXiv:0804.2896)
Bruch T., Read J., Baudis L., Lake G., 2008b, preprint (arXiv:0811.4172)
Bruch T., Peter A. H. G., Read J., Baudis L., Lake G., 2009, preprint (arXiv:0902.4001)
Clowe D., Bradač M., Gonzalez A. H., Markevitch M., Randall S. W., Jones C., Zaritsky D., 2006, ApJ, 648, L109
Conn B. C. et al., 2007, MNRAS, 376, 939
Dalcanton J. J., Bernstein R. A., 2002, AJ, 124, 1328
de Blok W. J. G., McGaugh S. S., Bosma A., Rubin V. C., 2001, ApJ, 552, L23
Debattista V. P., Moore B., Quinn T., Kazantzidis S., Maas R., Mayer L., Read J., Stadel J., 2008, ApJ, 681, 1076
Dehnen W., Binney J., 1998, MNRAS, 294, 429
Dunkley J. et al., 2009, ApJS, 180, 306
Fellhauer M. et al., 2006, ApJ, 651, 167
Feltzing S., Bensby T., 2008, Physica Scripta Vol. T, 133, 014031
Gill S. P. D., Knebe A., Gibson B. K., 2004, MNRAS, 351, 399
Gnedin O. Y., Kravtsov A. V., Klypin A. A., Nagai D., 2004, ApJ, 616, 16
Gottlöber S., Klypin A., Kravtsov A. V., 2001, ApJ, 546, 223
Governato F., Willman B., Mayer L., Brooks A., Stinson G., Valenzuela O., Wadsley J., Quinn T., 2007, MNRAS, 374, 1479
Governato F., Mayer L., Brook C., 2008a, in Funes J. G., Corsini E. M., eds, ASP Conf. Ser. Vol. 396, The Formation of Galaxy Disks. Astron. Soc. Pac., San Francisco, p. 453
Governato F. et al., 2008b, preprint (arXiv:0812.0379)
Holmberg J., Flynn C., 2000, MNRAS, 313, 209
Ibata R. A., Gilmore G., Irwin M. J., 1994, Nat, 370, 194
Johnston K. V., Law D. R., Majewski S. R., 2005, ApJ, 619, 800
Jungman G., Kamionkowski M., Griest K., 1996, Phys. Rep., 267, 195
Jurić M. et al., 2008, ApJ, 673, 864
Kamionkowski M., Koushiappas S. M., 2008, Phys. Rev. D, 77, 103509
Kampczyk P. et al., 2007, ApJS, 172, 329
Kazantzidis S., Kravtsov A. V., Zentner A. R., Allgood B., Nagai D., Moore B., 2004, ApJ, 611, L73
Kazantzidis S., Bullock J. S., Zentner A. R., Kravtsov A. V., Moustakas L. A., 2008, ApJ, 688, 254
Klypin A., Zhao H., Somerville R. S., 2002, ApJ, 573, 597
Kuhlen M., Diemand J., Madau P., 2008, ApJ, 686, 262
Lake G., 1989, AJ, 98, 1554
Macciò A. V., Dutton A. A., van den Bosch F. C., Moore B., Potter D., Stadel J., 2007, MNRAS, 378, 55
Majewski S. R., Skrutskie M. F., Weinberg M. D., Ostheimer J. C., 2003, ApJ, 599, 1082
March-Russell J., McCabe C., McCullough M., 2008, preprint (arXiv:0812.1931)
Mayer L., Governato F., Kaufmann T., 2008, Advanced Sci. Lett., 1, 7
Pedrosa S. E., Tissera P. B., Scannapieco C., 2009, MNRAS, 395, L211
Perryman M. A. C. et al., 2001, A&A, 369, 339
Pontzen A. et al., 2008, MNRAS, 390, 1349
Quinn P. J., Goodman J., 1986, ApJ, 309, 472
Read J. I., Wilkinson M. I., Evans N. W., Gilmore G., Kleyna J. T., 2006a, MNRAS, 367, 387
Read J. I., Wilkinson M. I., Evans N. W., Gilmore G., Kleyna J. T., 2006b, MNRAS, 366, 429
Read J. I., Saha P., Macciò A. V., 2007, ApJ, 667, 645
Read J. I., Lake G., Agertz O., Debattista V. P., 2008, MNRAS, 389, 1041
Romano-Diaz E., Shlosman I., Heller C., Hoffman Y., 2009, preprint (arXiv:0901.1317)
Scannapieco C., White S. D. M., Springel V., Tissera P. B., 2008, preprint (arXiv:0812.0976)
Springel V. et al., 2008, Nat, 456, 73
Stadel J., Potter D., Moore B., Diemand J., Madau P., Zemp M., Kuhlen M., Quilis V., 2008, preprint (arXiv:0808.2981)
Stinson G., Seth A., Katz N., Wadsley J., Governato F., Quinn T., 2006, MNRAS, 373, 1074
Vogelsberger M., White S. D. M., Helmi A., Springel V., 2008a, MNRAS, 385, 236
Vogelsberger M. et al., 2008b, preprint (arXiv:0812.0362)
Wadsley J. W., Stadel J., Quinn T., 2004, New Astron., 9, 137
Warnick K., Knebe A., 2006, MNRAS, 369, 1253
Widrow L. M., Dubinski J., 2005, ApJ, 631, 838
Zavala J., Okamoto T., Frenk C. S., 2008, MNRAS, 387, 364
Zemp M., Diemand J., Kuhlen M., Madau P., Moore B., Potter D., Stadel J., Widrow L., 2009, MNRAS, 394, 641

This paper has been typeset from a T_EX/L^AT_EX file prepared by the author.